Accelerating seismic interpolation with a gradient projection method based on tight frame property of curvelet

Jingjie Cao[1,4] Yanfei Wang[2] Benfeng Wang[3]

[1]Shijiazhuang University of Economics, Shijiazhuang, Hebei 050031, China.
[2]Key Laboratory of Petroleum Resources Research, Institute of Geology and Geophysics,
 Chinese Academy of Sciences, PO Box 9825, Beijing 100029, China.
[3]State Key Laboratory of Petroleum Resources and Prospecting, China University of Petroleum,
 Beijing 102249, China.
[4]Corresponding author. Email: cao18601861@163.com

Abstract.   Seismic interpolation, as an efficient strategy of providing reliable wavefields, belongs to large-scale computing problems. The rapid increase of data volume in high dimensional interpolation requires highly efficient methods to relieve computational burden. Most methods adopt the L_1 norm as a sparsity constraint of solutions in some transformed domain; however, the L_1 norm is non-differentiable and gradient-type methods cannot be applied directly. On the other hand, methods for unconstrained L_1 norm optimisation always depend on the regularisation parameter which needs to be chosen carefully. In this paper, a fast gradient projection method for the smooth L_1 problem is proposed based on the tight frame property of the curvelet transform that can overcome these shortcomings. Some smooth L_1 norm functions are discussed and their properties are analysed, then the Huber function is chosen to replace the L_1 norm. The novelty of the proposed method is that the tight frame property of the curvelet transform is utilised to improve the computational efficiency. Numerical experiments on synthetic and real data demonstrate the validity of the proposed method which can be used in large-scale computing.

Introduction

Seismic data that violates the Nyquist–Shannon sampling theorem may bring harmful aliases and deteriorate the results of migration, multiple elimination, de-noising, and AVO analysis (Liu, 2004; Naghizadeh and Sacchi, 2010). Seismic interpolation is a valid technique to enhance sampling density, by removing spatial aliasing and improving imaging accuracy (Spitz, 1991; Kreimer and Sacchi, 2013), and forms a crucial step in the seismic processing flow.

Many interpolation methods have been proposed in past decades, and signal processing based methods are the mainstream at present (Duijndam et al., 1999; Liu, 2004; Naghizadeh and Sacchi, 2010; Spitz, 1991). An important branch of these methods is the sparse transform based method combined with a regularisation strategy. For this method, seismic interpolation is treated as an inverse problem, and seismic events are assumed to be sparse in some transformed domain, such as the Fourier transform (Sacchi and Ulrych, 1996; Sacchi et al., 1998; Duijndam et al., 1999; Xu et al., 2005; Liu, 2004), or the linear Radon transform (Trad et al., 2002). Satisfactory results are obtained by these transforms under the assumption of linear events, while for curved evens, it should be dealt window by window. The curvelet transform, as a multi-scale and multi-directional transform, can represent curved events effectively and it can avoid the assumption of linear events (Herrmann and Hennenfent, 2008). Recently, seismic data interpolation methods

based on matrix/tensor completion have been proposed (Yang et al., 2012; Kreimer and Sacchi, 2012a, 2012b, 2013).

As a large-scale computing problem, seismic data interpolation requires efficient methods to reduce the increasing computational cost. Abma and Kabir (2006) introduced the projection onto convex sets (POCS) method to irregular seismic interpolation. Zwartjes and Sacchi (2007) adopted iterative-reweighted least-squares for interpolation. The iterative soft thresholding (IST) method was introduced by Herrmann and Hennenfent (2008). An improvement of the IST method, the fast iterative soft thresholding algorithm (FISTA), was recently proposed to alleviate the computational cost of the IST method. The spectral projected gradient for L_1 minimisation (SPGL1) method can obtain robust sparse solutions for L_1 constraint problems (van den Berg and Friedlander, 2009). These methods, however, are time consuming for the huge seismic data sets, therefore more efficient methods should be researched.

All the above methods use the L_1 norm to measure the sparsity of solutions, but the L_1 norm is non-differentiable at origin, and gradient-type methods cannot be applied directly. Researchers intend to solve the unconstrained L_1 norm regularisation, however, the regularisation parameter needs to be chosen carefully to obtain sparse solutions. In order to overcome the non-differentiability of the L_1 norm, some smooth functions are proposed to approximate it, then the gradient-based methods
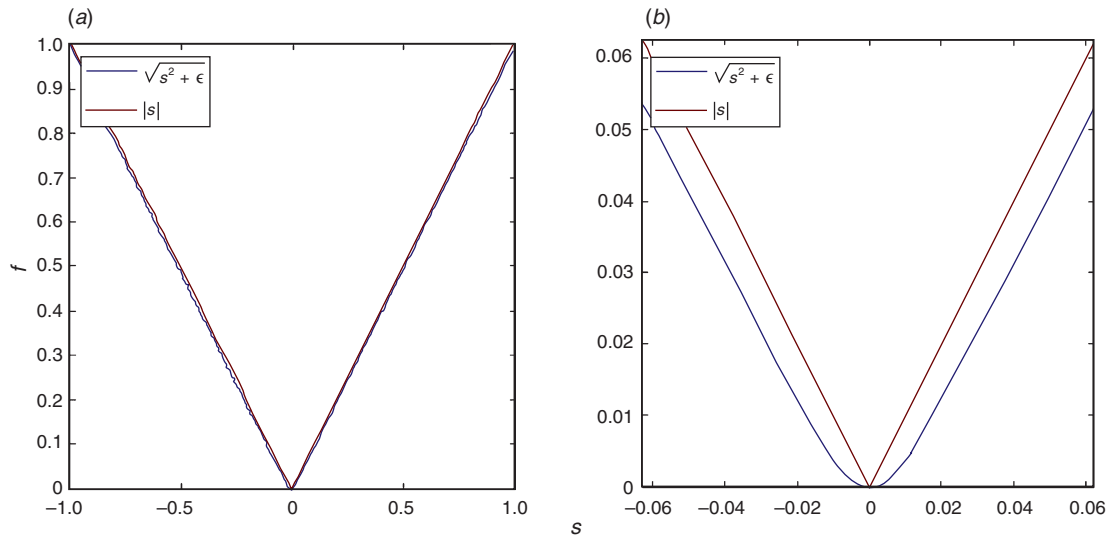
Fig. 1.   (*a*) $f_\varepsilon(s)$ with $\varepsilon = 0.0001$. (*b*) Magnified view of (*a*).
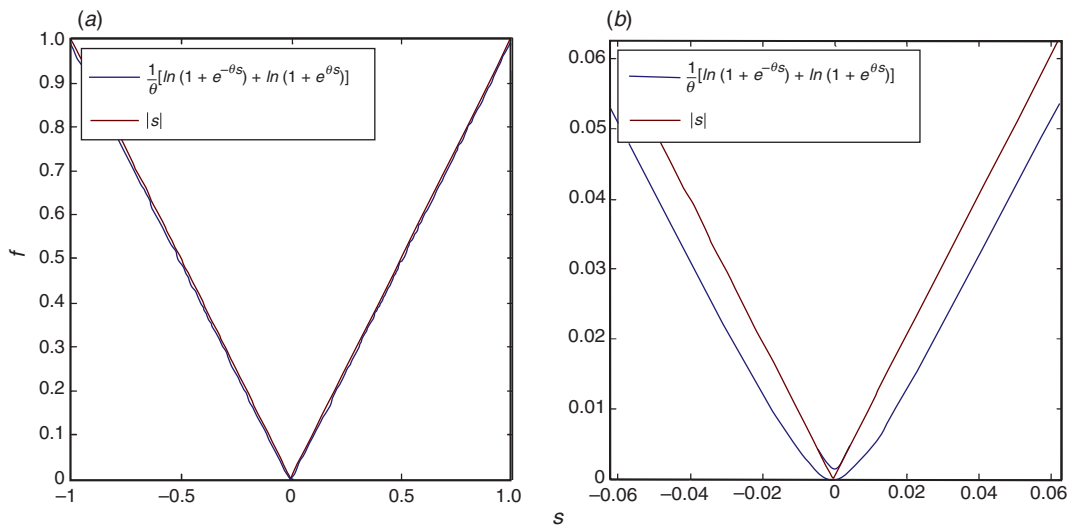

Fig. 2.   (*a*) $f_\theta(x)$ with $\theta = 10\,000$. (*b*) Magnified view of (*a*).
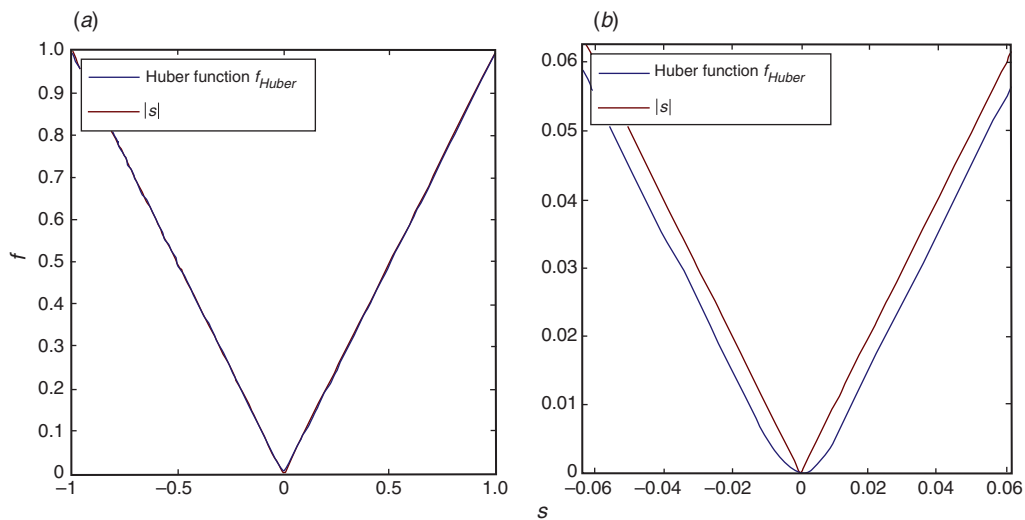

Fig. 3.   (*a*) $f_{Huber}(s)$ with $a = 0.0001$. (*b*) Magnified view of (*a*).
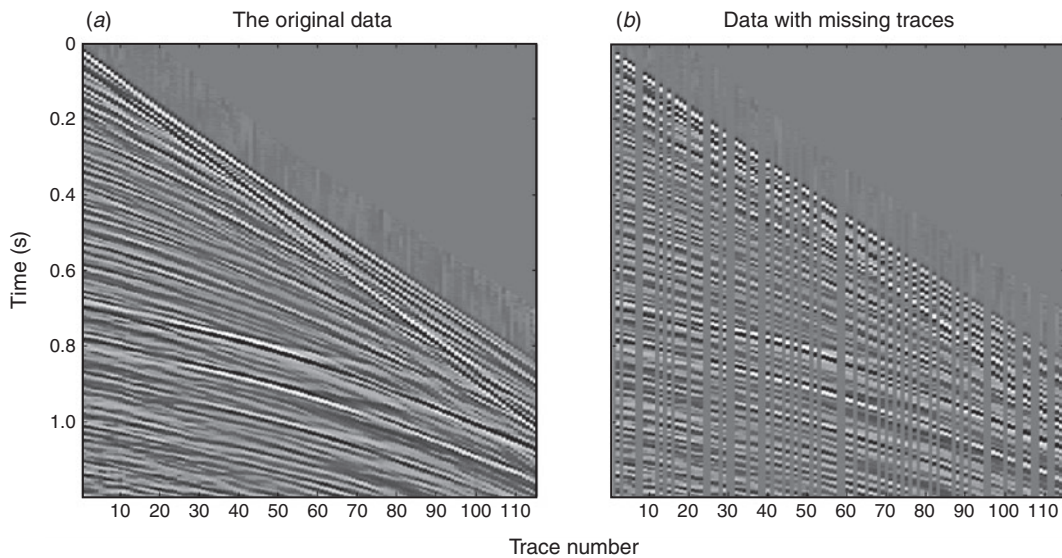
Fig. 4.   (*a*) Original shot data. (*b*) Sampled shot data.

Table 1.   Comparison of smooth L$_1$, FISTA and SPGL1 methods for shot data.

	Smooth L$_1$	FISTA	SPGL1
CPU time (s)	56	73	156
SNR (db)	10.4975	9.8556	9.9523
Relative error	0.2986	0.3215	0.3180

can be applied and the regularisation parameter is not required based on the gradient projection method with smooth L$_1$ norm approximation.

In this paper, some smooth L$_1$ norm functions are analysed first, then the Huber function is chosen to approximate the L$_1$ norm. A curvelet-based fast gradient projection method is proposed to solve the equality constrained smooth L$_1$ norm optimisation. The novelty of the proposed method is the use of the tight frame property of the curvelet transform to reduce the computational cost. Numerical examples on synthetic and real seismic data demonstrate the validity of the proposed method.

Sparse optimisation model of seismic interpolation

Mathematical model of seismic sparse interpolation

Seismic interpolation can be treated as an inverse problem, and the forward problem can be denoted as

$$\Phi x = b, \tag{1}$$

where Φ denotes the sampling processing, x is the complete seismic data, and b is the sampled data. There are infinitely many solutions theoretically, but we can utilise some prior information to find the solutions with physical meaning. Sparsity of the seismic data in a transformed domain is commonly used because seismic events can be sparsely expressed by some transforms. For seismic processing, some familiar transforms are the Fourier transform (Liu, 2004; Zwartjes and Sacchi, 2007), the linear Radon transform (Trad et al., 2002), the parabolic Radon transform (Darche, 1990) and the curvelet transform (Herrmann and Hennenfent, 2008). Recently, Gaussian beams have been adopted for seismic data decomposition (Liu et al.,
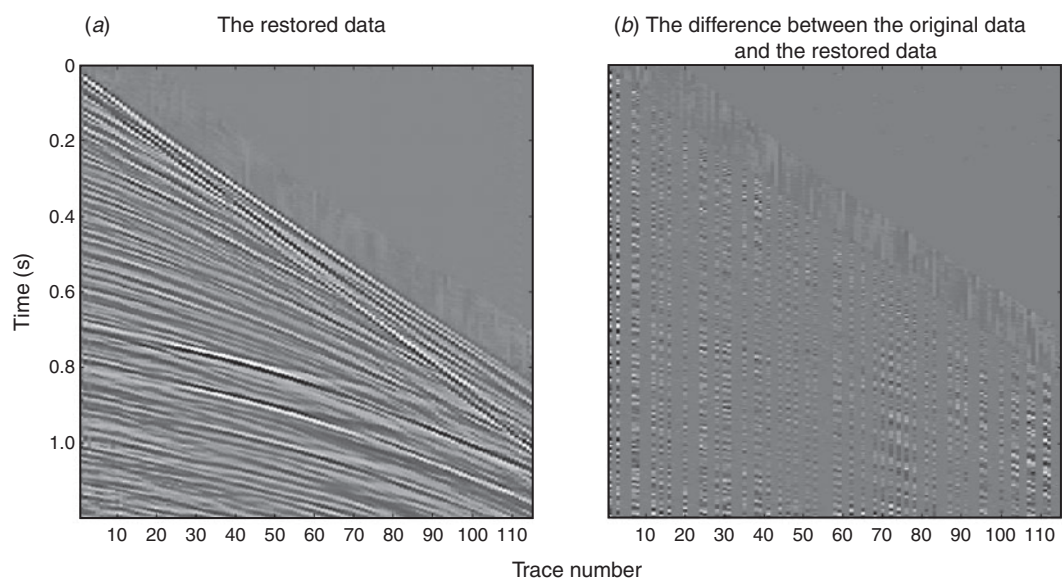

Fig. 5.   (*a*) Interpolation of shot data by smooth L$_1$ method. (*b*) Difference between (*a*) and original shot data.

2013; Wang et al., 2013). If $s = \Psi x$ is sparse, where Ψ is an orthogonal transform or tight frame, equation 1 can be changed to

$$\Phi x = \Phi \Psi^* s = A s = b, \tag{2}$$

where Ψ^* is the Hermitian transpose of Ψ and $A = \Phi \Psi^*$. Many methods have been developed to find sparse solutions to equation 2, such as greedy algorithms (Mallat and Zhang, 1993), convex optimisation (Beck and Teboulle, 2009; van den Berg and Friedlander, 2009; Chen et al., 1998) and non-convex optimisation (Mohimani et al., 2009). Convex optimisation methods with theoretically rigorous justification are suitable for large-scale computation (Cao et al., 2012; Chen et al., 1998). The most commonly used convex optimisation is the basis pursuit problem:

$$\min \|s\|_1 \ \text{s.t.} A s = b, \tag{3}$$

which can be transformed into linear optimisation and solved by the interior point method (Chen et al., 1998; Candes and Tao,

2005). Because the objective function of equation 3 is non-differentiable at origin, it cannot be solved by the conjugate gradient method and Newton-type methods directly. Hence, researchers have proposed to solve the unconstrained form of equation 3:

$$\min \|A s - b\|_2^2 + \lambda \|s\|_1, \tag{4}$$

using for example the IST and FISTA methods, but the regularisation parameter λ should be adjusted carefully. Another strategy to overcome the non-differentiability of equation 3 is replacing the L_1 norm by its smooth approximations, which can be called the smooth L_1 method. Thus, equation 3 can be changed into

$$\min F(s) \text{s.t.} A s = b, \tag{5}$$

where $F(s)$ is a smooth approximation of the L_1 norm. In the following, some smooth L_1 norm functions are discussed and analysed.
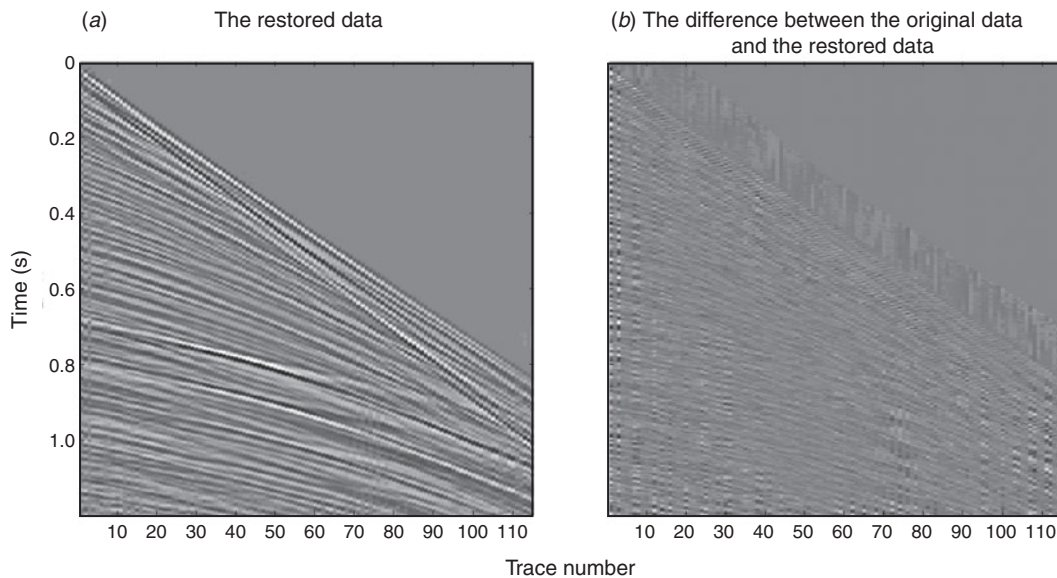

Fig. 6. (*a*) Interpolation of shot data by FISTA method. (*b*) Difference between (*a*) and original shot data.
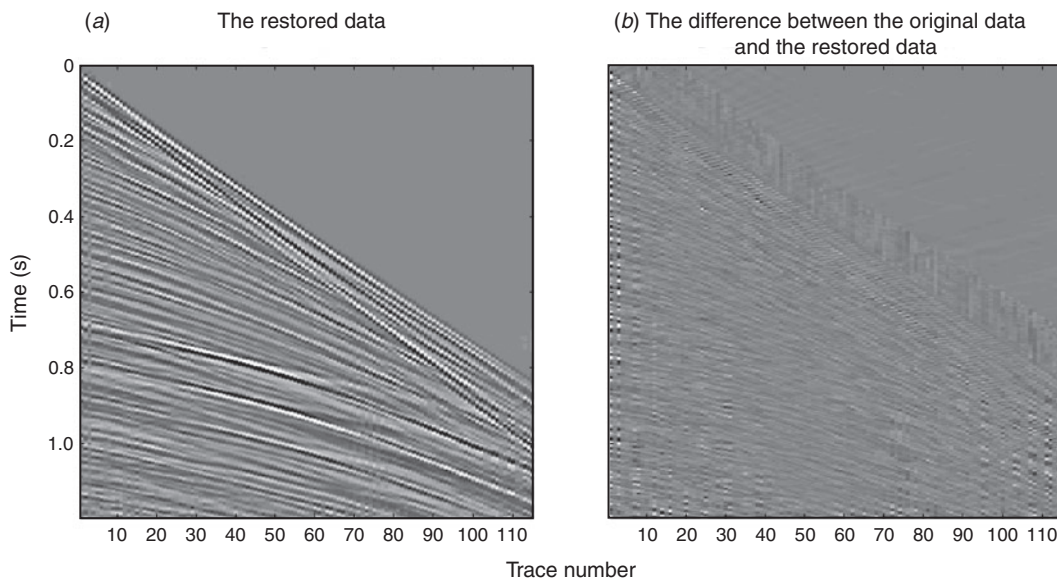

Fig. 7. (*a*) Interpolation of shot data by SPGL1 method. (*b*) Difference between (*a*) and original shot data.

Comparison of smooth L_1 norm functions

Smooth L_1 norm functions are smooth approximations of the L_1 norm which are separable and can be written as $F(s)=\sum_{i=1}^{N}f(s_i)$, so we just need to analyse the 1D case $f(s)$, where s is a scalar. The first function we discuss is

$$f_\varepsilon(s) = \sqrt{s^2 + \varepsilon} \qquad (6)$$

As a continuous, convex and differential function (Wang et al., 2011), it approximates to $|s|$ very well when ε is very small. Figure 1a plots this function with $\varepsilon = 0.0001$. However, it is not zero exactly at the original point; a magnified view (Figure 1b) shows the deficiency clearly. This may affect the sparsity of solutions.

The second function is

$$f_\theta(s) = \frac{1}{\theta}[\ln(1 + e^{-\theta s}) + \ln(1 + e^{\theta s})], \qquad (7)$$

which approximates to $|s|$ very well when θ is large enough. This function is convex and differential (Chen and Mangasarian,

1996). A plot of it is given in Figure 2a with $\theta = 10\,000$. Figure 2b is a magnified view of Figure 2a. As with Figure 1b, it is also non-zero at the original point.

Another familiar function is the Huber function:

$$f_{\text{Huber}}(s) = \begin{cases} s^2/2a, & \text{if } |s| \leq a \\ |s| - a/2, & \text{else } |s| > a \end{cases}. \qquad (8)$$

In equation 8, a is called a super-parameter. The Huber function is smooth everywhere and approaches to $|s|$ extremely well when a turns to zero (Bube and Nemeth, 2007). It is plotted in Figure 3a with $a = 0.0001$; a magnified view shows that it equals zero exactly at the original point. The Huber function is a hybrid of the L_1 norm and the L_2 norm; it behaves like the L_2 norm for small a and like the L_1 norm for large a. The smooth transition from L_2 norm to L_1 norm behaviour is controlled by a. Huber functions are not new in geophysical inverse problems; Sacchi used the Cauchy function and Huber functions for deconvolution to get sparse reflectivity series (Sacchi, 1997). Here, we take it as a measurement to get sparse solutions of seismic interpolation.
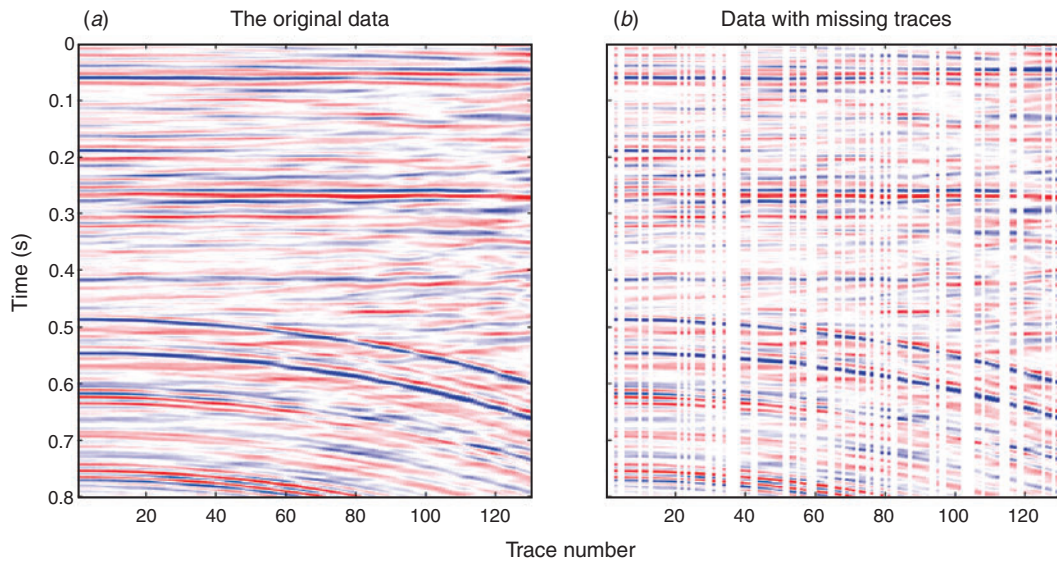

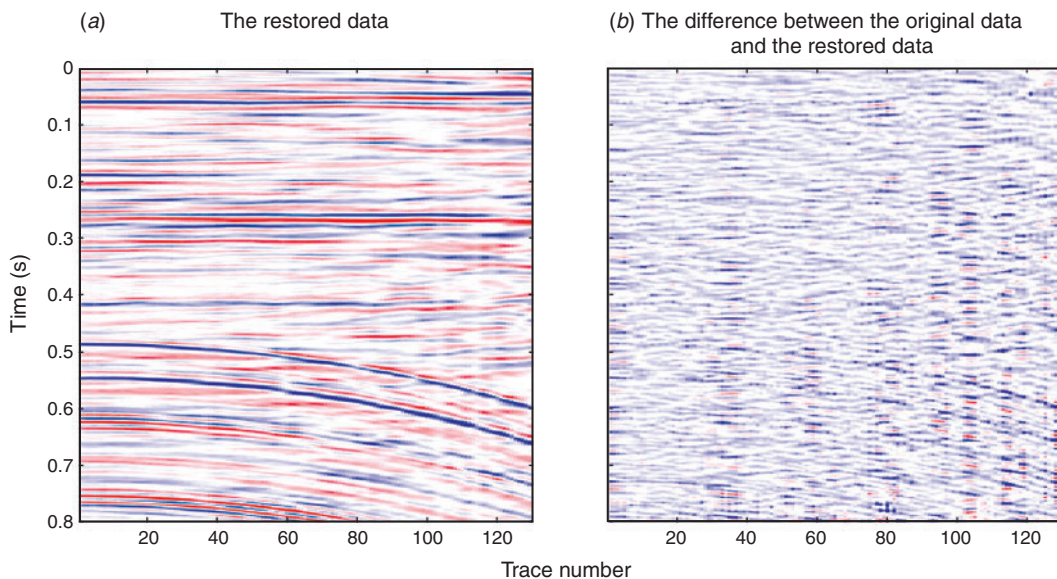**Fig. 8.** (*a*) Original poststack data. (*b*) Sampled poststack data.

Fig. 9. (*a*) Interpolation of poststack data by smooth L_1 method. (*b*) Difference between (*a*) and original poststack data.

Based on the above discussions, some conclusions can be made: (1) A super-parameter exists in each function to control the approximation to $|s|$, and they are all differential; (2) $f_\varepsilon(s)$ and $f_\theta(x)$ are not exactly zero at the original point, while $f_{\mathrm{Huber}}(s)$ equals zero at the original point and can approach to the L_1 norm better for given proper parameters. Therefore, $f_{\mathrm{Huber}}(s)$ is chosen as the L_1 norm approximation. Rewriting equation 5 using the $f_{\mathrm{Huber}}(s)$ constraint yields

$$\min F(s) := \sum_{i=1}^{N} f_{\mathrm{Huber}}(s_i) \quad \text{s.t.} As = b. \tag{9}$$

Equation 9 is always transformed into an unconstraint problem, in which the regularisation factor should be chosen carefully. In order to avoid the regularisation factor, the gradient projection method, which is a very efficient strategy, is used to solve the constrained optimisations.

Gradient projection method for smooth L_1 norm optimisation

Since equation 2 is underdetermined, $s = \{s|As = b\}$ is a convex set, thus equation 9 can be solved by a convex set projection method. A gradient projection algorithm for equation 9 is designated as follows:

Algorithm

*Step 1.* Give the maximum iteration L, the parameter $a = 0.0001$, $k = 0$, and the initial solution s_0.

Step 2. Solve the gradient $\nabla F(s_k)$. If the stopping criterion is satisfied, go to Step 4; otherwise, give a trial iteration $s_{k+1}^{pre} = s_k - \mu \nabla F(s_k)$, where μ is the step length (which can be solved by back-tracing method).

Step 3. Update the iteration point: $s_{k+1} = s_{k+1}^{pre} - P_s(s_{k+1}^{pre})$ ($P_s(s_{k+1}^{pre})$ i.e. projection onto $s = \{s|As = b\}$), let $s_k = s_{k+1}$, $k = k+1$, and return to Step 2.

Step 4. Give the final solution: $s = s_k$.
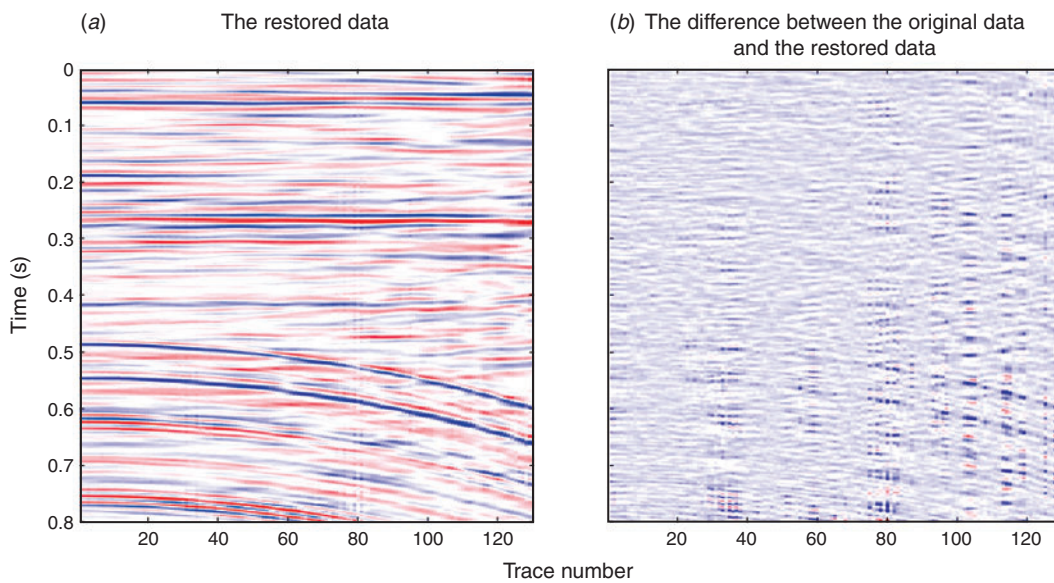
Fig. 10. (*a*) Interpolation of poststack data by FISTA method. (*b*) Difference between (*a*) and original poststack data.
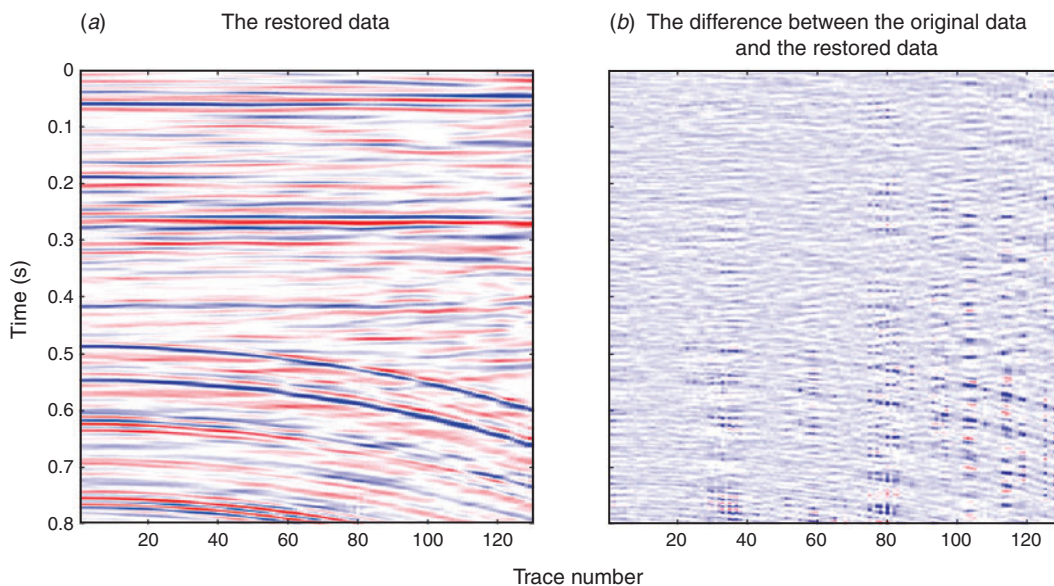
Fig. 11. (*a*) Interpolation of poststack data by SPGL1 method. (*b*) Difference between (*a*) and original poststack data.

Table 2. Comparison of smooth L$_1$, FISTA and SPGL1 methods for post-stack data

	Smooth L$_1$	FISTA	SPGL1
CPU time (s)	56	80	163
SNR (db)	22.1805	22.7094	22.9518
Relative error	0.0778	0.0732	0.0712

We choose the stopping criterion as the discrepancy principle (Wang et al., 2011). The initial solution is $s = A^*b$, where A^* is the Hermitian transpose of A.

The main computations of this algorithm are focused on Step 3, because the projection in Step 3, $P_s(s_{k+1}^{pre}) = A^*(AA^*)^{-1}(As_{k+1}^{pre} - b)$, contains a curvelet transform, an inverse curvelet and a large-scale matrix inversion. However, if the inversion of AA^* can be omitted, the algorithm will enhance computation efficiency significantly. A curvelet transform as the sparse transform is selected here, because it is not only an excellent sparse transform but also a tight frame, based on which AA^* can be simplified to the identify matrix. Then, projections can be simplified to $P_s(s_{k+1}^{pre}) = A^*(As_{k+1}^{pre} - b)$. Properties of the curvelet transform will be introduced briefly in the following section.

Cao et al. (2012) proposed a smooth L$_0$ method for seismic interpolation; however, there are two-level iterations in the smooth L$_0$ method, and parameters of smooth L$_0$ function and iteration should be changed carefully to prevent getting local solutions. The gradient projection method presented above only needs one-level iteration and the super-parameter a of the Huber function is fixed and need not be adjusted.

The curvelet transform

Because of the excellent sparse expression ability of curvelet for seismic data, it has received extensive application in seismic processing. As an anisotropic, multi-directional, multi-scale and local frame (Candes, 2006; Candes and Donoho, 2004), the curvelet transform has been proved to be the sparsest among the existing transforms for seismic data (Herrmann and Hennenfent, 2008). The discrete form of curvelet can be written as $s = \Psi x$, where s is a vector denoting the discrete set of curvelet coefficients, x is the discrete form of the data, and Ψ is the curvelet transform matrix. Besides the excellent compression for seismic data, the curvelet transform creates a tight frame by wrapping, which can perfectly reconstruct data after decomposition by applying the transpose of the curvelet transform; that is, $x = \Psi^*\Psi x$ for an arbitrary finite-energy vector x (Herrmann and Hennenfent, 2008), thus $\Psi^*\Psi x = I$. Based on this property, $AA^* = \Phi\Psi^*\Psi\Phi = I$. This property can then be used to accelerate the algorithm significantly.

Numerical examples

The performance of the proposed method is evaluated on two real data experiments, though more examples performed can also show similar results. A shot data experiment is given at first to prove its ability for field data, then application on post-stack seismic data also verify the validity of the proposed method. To further demonstrate the efficiency of the proposed method, comparisons are conducted with the FISTA and SPGL1 methods.

Shot data experiment

A shot data interpolation is implemented to test the ability of the proposed smooth L$_1$ method. The receiver interval is 12.5 m in the shot gather with a 2 ms time sampling interval. The dataset contains 115 traces with 600 time samples per trace. The incomplete acquisition was simulated by a random sample of 69 traces. The original data is given in Figure 4a, and the sampled data is given in Figure 4b. We made experiments by using the smooth L$_1$, FISTA (Beck and Teboulle, 2009) and SPGL1 methods (van den Berg and Friedlander, 2009). Some parameters in each algorithm are listed below: the max-iteration number is 15 for the smooth L$_1$ method, 20 for FISTA, and 30 for SPGL1. Based on the above parameters, these methods can obtain similar results with much different CPU times. The CPU time, signal-to-noise ratio (SNR) and relative error are listed in Table 1, where the SNR is defined as:

$$SNR = 10\log_{10}\frac{\|d_{\text{orig}}\|_2^2}{\|d_{\text{orig}} - d_{\text{rest}}\|_2^2}$$

where d_{orig} is the original data and d_{rest} is the restored data, and the relative error is defined as

$$\frac{\|d_{\text{orig}} - d_{\text{rest}}\|_2}{\|d_{\text{orig}}\|_2}$$

The interpolation result by the smooth L$_1$ is given in Figure 5a and the difference between it and the original data is shown in Figure 5b; results from the FISTA method and its difference from the original data are shown in Figure 6; interpolation using the SPGL1 method and the difference between the restoration and the original data are shown in Figure 7. From Table 1, we can conclude that the smooth L$_1$ method is faster than FISTA and approximately one third of the CPU time of the SPGL1 method.

Post-stack seismic data experiment

We further examine the efficiency of the smooth L$_1$ method with post-stack data. A post-stack section is given in Figure 8a which consists of 130 traces with a trace interval of 25 m and 401 time samples pre-trace with 2 ms as the time interval. The subsampled gather is shown in Figure 8b with 40% of the original traces randomly deleted. The maximum iteration number of the smooth L$_1$ method is 20; the interpolation of the smooth L$_1$ method and the difference between the interpolation and the original data are displayed in Figure 9, while the interpolation results using the FISTA with a maximum iteration of 30 and its difference from the original data are shown in Figure 10. Interpolation based on SPGL1 with a maximum iteration of 50 and its difference from the original data are shown in Figure 11. The CPU time, SNR and relative error of these methods are shown in Table 2. These results also show that, when the interpolation results are almost the same, the smooth L$_1$ method is faster than the FISTA method and approximately one third of the CPU time of the SPGL1 method. Thus, the proposed method is efficient and can reduce the computational time and cost significantly. We also performed several examples and all of them can verify the efficiency of the smooth L$_1$ method; these are not listed here because of the limited space.

Conclusion

In this paper, a fast gradient projection method for smooth L$_1$ optimisation based on tight frame property of curvelet is proposed. Some smooth functions as L$_1$ norm approximation are presented and analysed, then the Huber function is chosen as the best approximation to the L$_1$ norm among those listed. The tight frame property with bound 1 of the curvelet transform is used to accelerate the method. The proposed method overcomes the non-differentiability of the L$_1$ norm and does not need to choose a classical regularisation parameter. Comparison of the proposed method with some state-of-the-art sparse methods, such as the FISTA and SPGL1 methods, by experiments indicate that the

proposed method is the fastest among the three methods. Therefore, it can be used to improve the efficiency of seismic processing, especially for high dimensional seismic data interpolation.

The proposed method is based on the curvelet transform to obtain the interpolated seismic data which is a redundancy transform and is time consuming, therefore unsuitable for large gaps. Future research on more efficient sparse transforms (Trad, 2009), especially efficient high dimensional transforms, is required. The L_1 norm constraint and its smooth approximation are discussed in this paper and it is found not to be the best sparse constraint. Therefore, other sparse constraints, like the L_p norm ($0 < P < 1$) should be investigated further.

Acknowledgments

References

Abma, R., and Kabir, N., 2006, 3D interpolation of irregular data with a POCS algorithm: *Geophysics*, **71**, E91–E97. doi:10.1190/1.2356088

Beck, A., and Teboulle, M., 2009, A fast iterative shrink-thresholding algorithm for linear inverse problems: *SIAM Journal on Imaging Sciences*, **2**, 183–202. doi:10.1137/080716542

Bube, K., and Nemeth, T., 2007, Fast line searches for the robust solution of linear systems in the hybrid and Huber norms: *Geophysics*, **72**, A13–A17. doi:10.1190/1.2431639

Candes, E., 2006, Compressive sampling: *Proceedings of the International Congress of Mathematicians*: European Mathematical Society Publishing House, 33–52.

Candes, E., and Donoho, D., 2004, New tight frames of curvelets and optimal representations of objects with piecewise singularities: *Communications on Pure and Applied Mathematics*, **57**, 219–266. doi:10.1002/cpa.10116

Candes, E., and Tao, T., 2005, Decoding by linear programming: *IEEE Transactions on Information Theory*, **51**, 4203–4215. doi:10.1109/TIT.2005.858979

Cao, J., Wang, Y., and Yang, C., 2012, Seismic data restoration based on compressive sensing using regularization and zero-norm sparse optimization: *Chinese Journal of Geophysics*, **55**, 239–251. doi:10.1002/cjg2.1718

Chen, C., and Mangasarian, O., 1996, A class of smoothing functions for non-linear and mixed complementarity problems: *Computational Optimization and Applications*, **5**, 97–138. doi:10.1007/BF00249052

Chen, S., Donoho, D., and Saunders, M., 1998, Atomic decomposition by basis pursuit: *SIAM Journal on Scientific Computing*, **20**, 33–61. doi:10.1137/S1064827596304010

Darche, G., 1990, Spatial interpolation using a fast parabolic transform: 60th Annual International Meeting, SEG, Expanded Abstracts, 1647–1650.

Duijndam, A., Schonewille, M., and Hindriks, C., 1999, Reconstruction of band-limited signals, irregularly sampled along one spatial direction: *Geophysics*, **64**, 524–538. doi:10.1190/1.1444559

Herrmann, F., and Hennenfent, G., 2008, Non-parametric seismic data recovery with curvelet frames: *Geophysical International*, **173**, 233–248. doi:10.1111/j.1365-246X.2007.03698.x

Kreimer, N., and Sacchi, M., 2012a, A tensor higher-order singular value decomposition (HOSVD) for pre-stack seismic data noise-reduction and interpolation: *Geophysics*, **77**, V113–V122. doi:10.1190/geo2011-0399.1

Kreimer, N., and Sacchi, M., 2012b, Reconstruction of seismic data via tensor completion: *IEEE Statistical Signal Processing Workshop (SSP)*, 29–32.

Kreimer, N., and Sacchi, M., 2013, Tensor completion based on nuclear norm minimization for 5D seismic data reconstruction: *Geophysics*, **78**, V273–V284. doi:10.1190/geo2013-0022.1

Liu, B., 2004, Multi-dimensional reconstruction of seismic data: Ph.D. thesis, University of Alberta.

Liu, P., Wang, Y. F., Yang, M. M., and Yang, C. C., 2013, Seismic data decomposition using sparse Gaussian beams: *Chinese Journal of Geophysics*, **56**, 3887–3895.

Mallat, S., and Zhang, Z., 1993, Matching pursuits with time-frequency dictionaries: *IEEE Transactions on Signal Processing*, **41**, 3397–3415. doi:10.1109/78.258082

Mohimani, H., Babaie-Zadeh, M., and Jutten, C., 2009, A fast approach for over-complete sparse decomposition based on smoothed l^0 norm: *IEEE Transactions on Signal Processing*, **57**, 289–301. doi:10.1109/TSP.2008.2007606

Naghizadeh, M., and Sacchi, M., 2010, Beyond alias hierarchical scale curvelet interpolation of regularly and irregularly sampled seismic data: *Geophysics*, **75**, WB189–WB202. doi:10.1190/1.3509468

Sacchi, M., 1997, Re-weighting strategies in seismic deconvolution: *Geophysical Journal International*, **129**, 651–656. doi:10.1111/j.1365-246X.1997.tb04500.x

Sacchi, M. D., and Ulrych, T. J., 1996, Estimation of the discrete Fourier transform, a linear inversion approach: *Geophysics*, **61**, 1128–1136. doi:10.1190/1.1444033

Sacchi, M., Ulrych, T., and Walker, C., 1998, Interpolation and extrapolation using a high resolution discrete Fourier transform: *IEEE Transactions on Signal Processing*, **46**, 31–38. doi:10.1109/78.651165

Spitz, S., 1991, Seismic trace interpolation in the F-X domain: *Geophysics*, **56**, 785–794. doi:10.1190/1.1443096

Trad, D., 2009, Five-dimensional interpolation: recovering from acquisition constraints: *Geophysics*, **74**, V123–V132. doi:10.1190/1.3245216

Trad, D., Ulrych, T., and Sacchi, M., 2002, Accurate interpolation with high-resolution time-variant Radon transforms: *Geophysics*, **67**, 644–656. doi:10.1190/1.1468626

van den Berg, E., and Friedlander, M. P., 2009, Probing the Pareto frontier for basis pursuit solutions: *SIAM Journal on Scientific Computing*, **31**, 890–912. doi:10.1137/080714488

Wang, Y., Cao, J., and Yang, C., 2011, Recovery of seismic wavefields based on compressive sensing by an l_1-norm constrained trust region method and the piecewise random sub-sampling: *Geophysical Journal International*, **187**, 199–213. doi:10.1111/j.1365-246X.2011.05130.x

Wang, Y, Liu, P, Li, Z, Sun, T, Yang, C, and Zheng, Q, 2013, Data regularization using Gaussian beams decomposition and sparse norms: *Journal of Inverse and Ill-Posed Problems*, **21**, 1–23. doi:10.1515/jip-2012-0030

Xu, S., Zhang, Y., Pham, D., and Lambare, G., 2005, Anti-leakage Fourier transform for seismic data regularization: *Geophysics*, **70**, V87–V95. doi:10.1190/1.1993713

Yang, Y., Ma, J., and Osher, S., 2012, Seismic data reconstruction via matrix completion: UCLA CAM Report, 12–14.

Zwartjes, P., and Sacchi, M., 2007, Fourier reconstruction of nonuniformly sampled, aliased seismic data: *Geophysics*, **72**, V21–V32. doi:10.1190/1.2399442